Advanced Experimental Methods : Fluid

Data-driven modal decompositions

Luc Pastur

ENSTA Paris

Flow structures

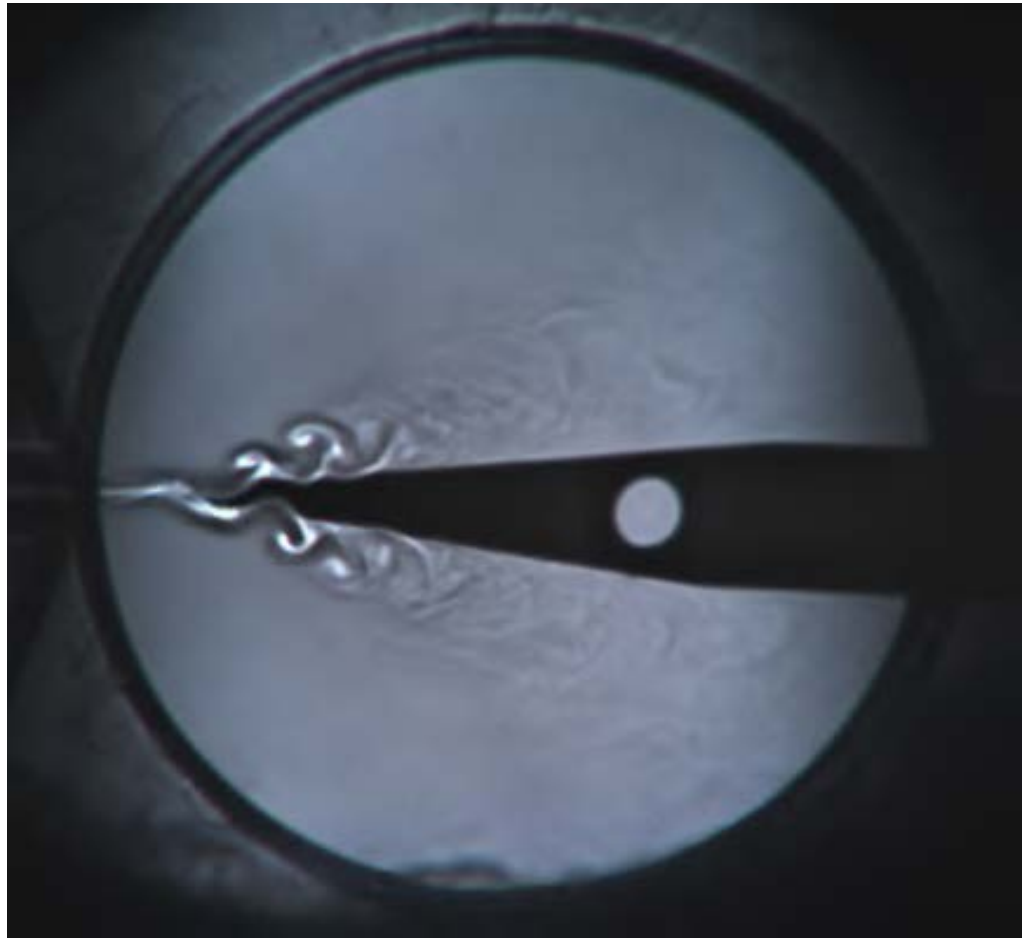

Bevel sound

Flow structures

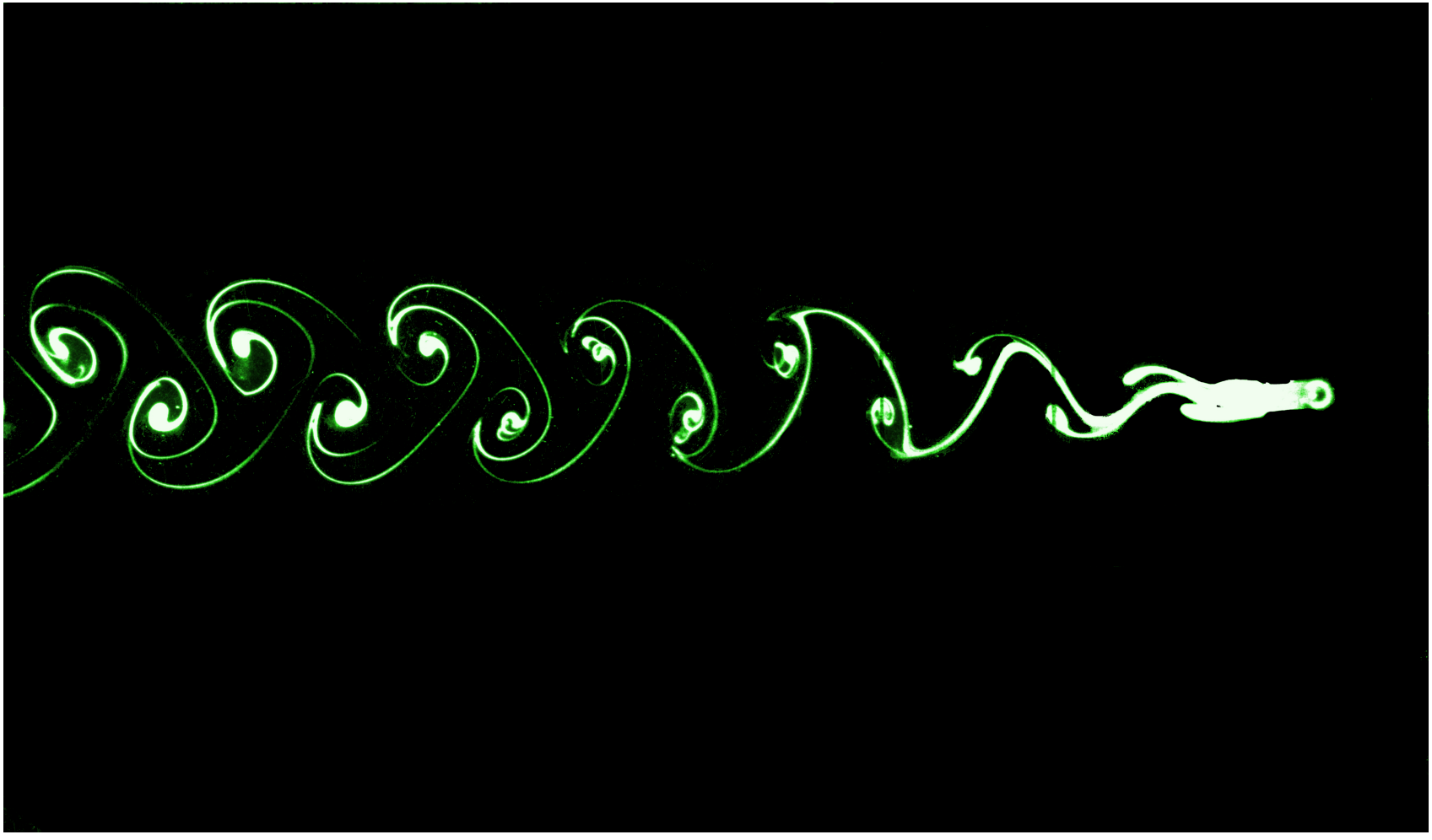

Cylinder wake flow

Flow structures

Guadeloupe wake flow

Flow structures

Wing stall flow

Flow structures

Natural convection
(Schlieren photograph, Gas Dynamics Lab, Penn State University)

Flow structures

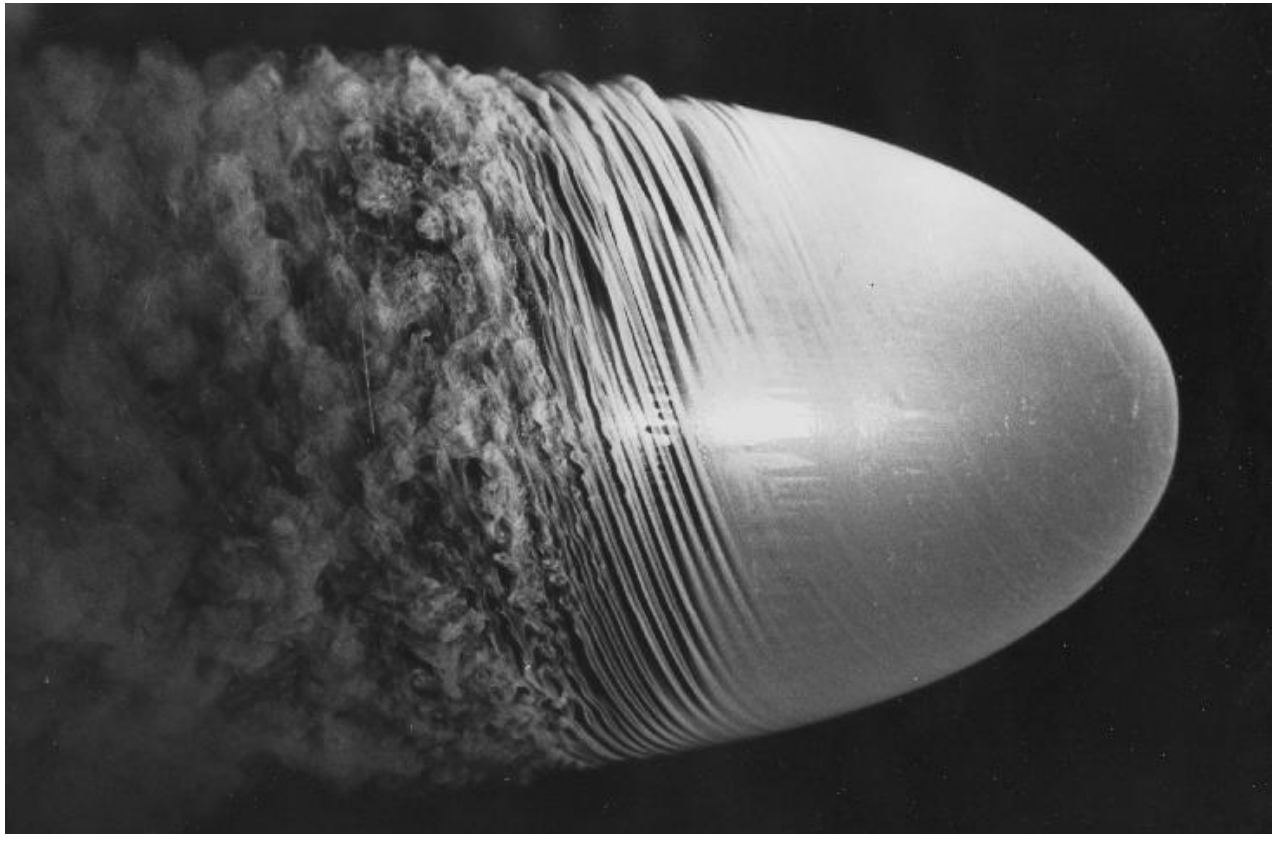

Boundary layer transition

Flow structures

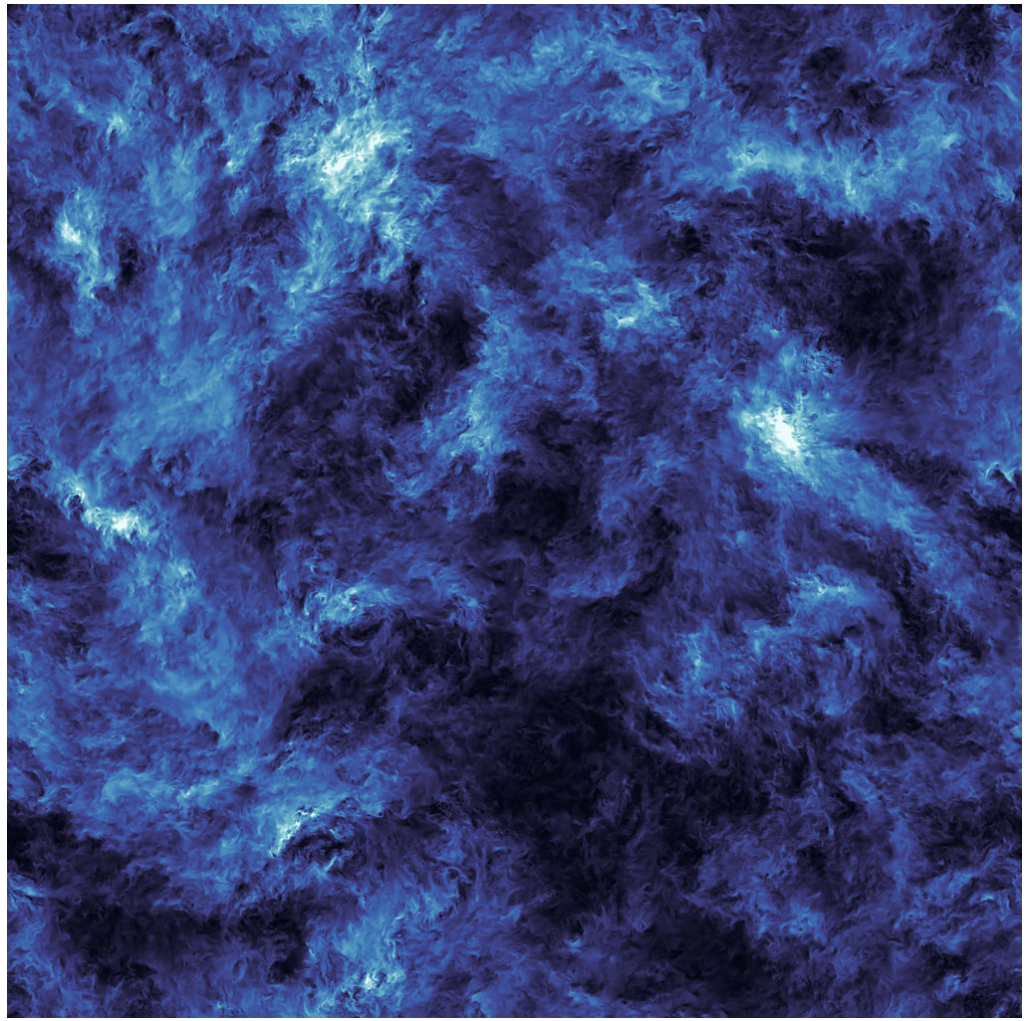

Fully developed turbulence
(computer simulation with more than 200 billion degrees of freedom,
M. Wilczek (2018))

How to extract flow structures ?

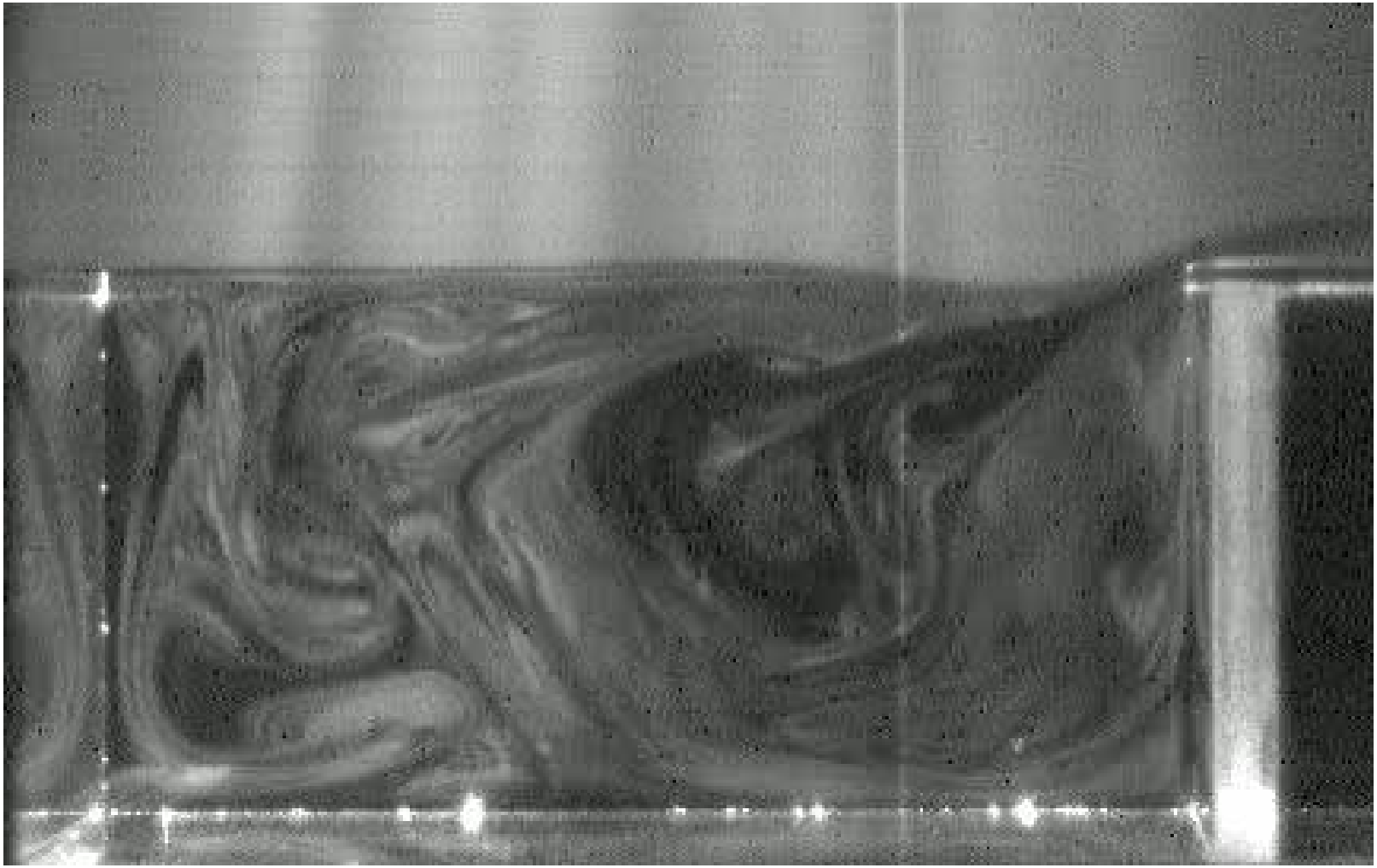

Open cavity flow

Decomposition on a basis of known functions

The usual approach is to decompose the flow on a basis of known functions (in the L^2-space) :

- Fourier mode expansion $\exp(\mathrm{i}\,\mathbf{k}\cdot\mathbf{r})$;
- Bessel functions (in axisymmetric geometries) ;
- Wavelets (redundant decomposition for scanning both location and scale of a given pattern in the flow) ;
- Global modes (given by the stability analysis of a steady base flow) ;
- Etc

Seeding thoughts

Holmes, P. J., Lumley, J. L., Berkooz, G., Mattingly, J. C., & Wittenberg, R. W., Physics Reports 287 (1997) 337-384

For fluid flow one has a well-accepted mathematical model : the Navier-Stokes equations. Why, then, is the problem of turbulence so intractable ? One major difficulty is that the equations appear insoluble in any reasonable sense. (A direct numerical simulation certainly yields a "solution", but it provides little understanding of the process per se.) However, three developments are beginning to bear fruit :

1. *The discovery, by experimental fluid mechanicians, of coherent structures in certain fully developed turbulent flows ;*
2. *the suggestion, by Ruelle, Takens and others, that strange attractors and other ideas from dynamical systems theory might play a role in the analysis of the governing equations, and*
3. *the introduction of the statistical technique of Karhunen-Loève or proper orthogonal decomposition, by Lumley in the case of turbulence.*

Toward data-driven bases of function ?

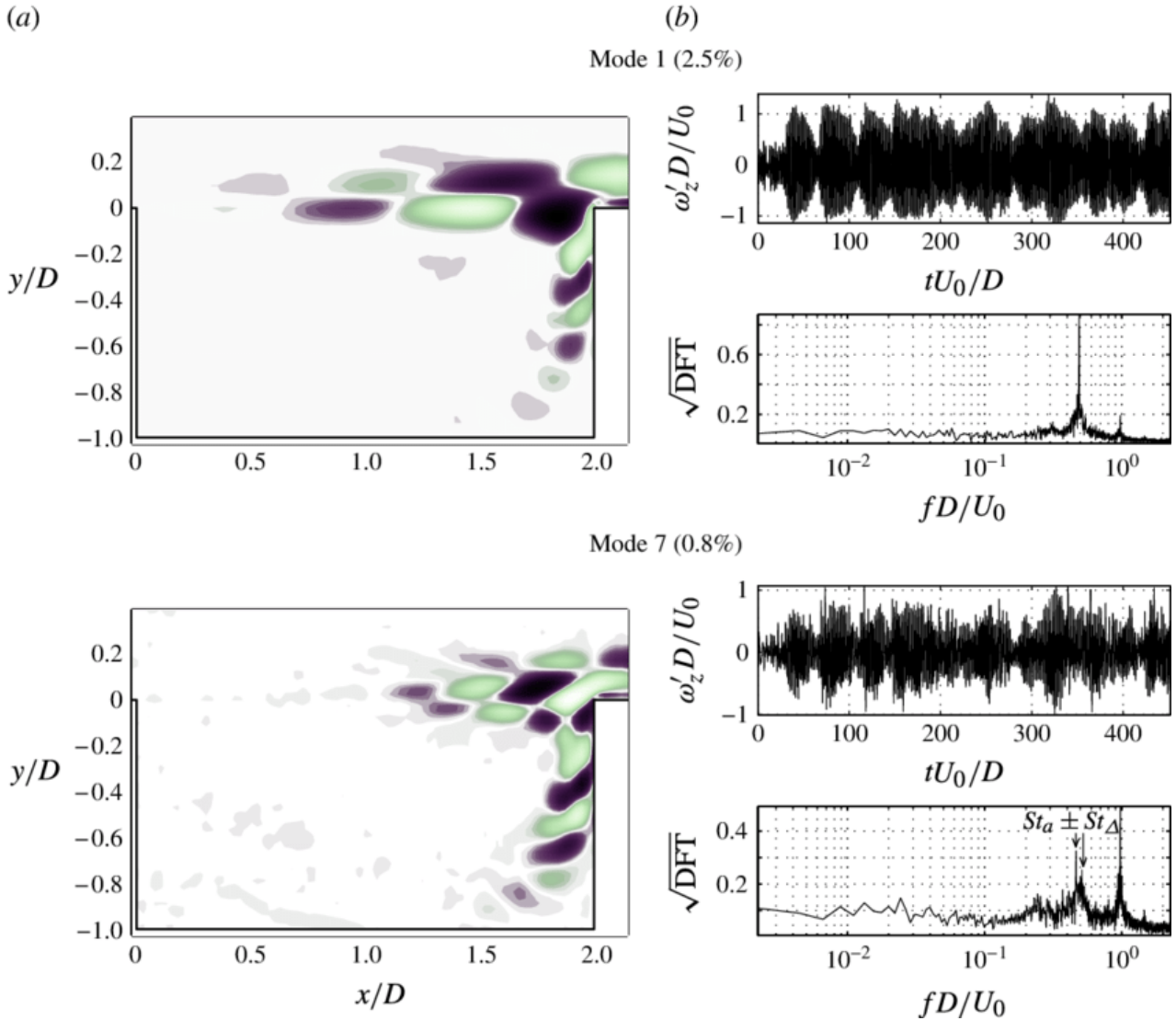

Open cavity flow coherent structures

Outline

Some preliminary definitions

Deterministic systems

We consider the state vector $\mathbf{X} \in M$ where $M \subset \mathbb{R}^N$ is the manifold on which evolves the system.
The dynamics is deterministic when the system can be written in the form

$$\dot{\mathbf{X}} = \mathbf{f}(\mathbf{X}, t).$$

The system is said autonomous when the vector field $\mathbf{f}$ does not depend explicitly on time t.

Example of deterministic systems :

- The pendulum
$$\ddot{y} + \omega_0^2 y = 0,$$
for which $\mathbf{X} = (X_1, X_2) = (y, \dot{y})^T$ and $\mathbf{f}(\mathbf{X}) = (X_2, -\omega_0^2 X_1)^T$.
- The diffusion equation
$$\partial\phi/\partial t = \nu \partial^2\phi/\partial x^2,$$
where $\mathbf{X}(t) = (\phi(x_1, t), \phi(x_2, t) \ldots)^T$ is of inifinite dimension.
- etc.

What about the Navier-Stokes equations ?

Flow field as realizations of the state vector

- If the sampling is random, $\mathbf{X}$ can be seen as a random process.
- $\mathbf{u}(\mathbf{X})$ is the result of a measurement on the random variable.
- We form the set of random variables $S = \{\mathbf{u}_k\}_{k=1,\dots,N}$ where $\mathbf{u}_k = \mathbf{u}(\mathbf{X}(t_k))$
- Can we define *principal components* $\{\psi_k\}_{k=1,\dots,N}$ "most representative" of the data in S ?

Probability functions

Let us consider the ensembles of scalar random variables $S_u = \{u_k\}_{k=1,\dots,N}$ and $S_v = \{v_k\}_{k=1,\dots,N}$. We note :

$\rightarrow$ $p(u)$ the probability function of the random variables : it focuses on what happens at 1 point regardless of the others ;

$\rightarrow$ $p(u, v)$ the joint probability function : it focuses on the link between two realizations, regardless of the others.

One-point statistics

- Mean

$$< u >_E = \int_S u\, p(u)\, du$$

- Variance

$$\sigma_u^2 = \left\langle (u - < u >_E)^2 \right\rangle_E = \int_S (u - < u >_E)^2\ p(u)\, du$$

Two-points statistics

- Auto-correlation

$$R_{uu}(n,m) = < u_n u_m >_E = \int_S u_n u_m \, p(u_n, u_m) \, du_n \, du_m$$

- Auto-covariance

$$C_{uu}(n,m) = \langle (u_n - < u_n >_E)(u_m - < u_m >_E) \rangle_E$$

- Cross-correlation

$$R_{uv}(n,m) = < u_n v_m >_E = \int_S u_n v_m \, p(u_n, v_m) \, du_n \, dv_m$$

- Cross-covariance

$$C_{uv}(n,m) = \langle (u_n - < u_n >_E)(v_m - < v_m >_E) \rangle_E$$

Note :

$$\text{Variance } C_{uu}(n,n) = \sigma_u^2.$$
$$\text{Correlation } R_{uv}(n,n) = \mathrm{corr}(u_n, v_n)$$
$$\text{Covariance } C_{uv}(n,n) = \mathrm{cov}(u_n, v_n)$$

Two-point correlations of the velocity field

Consider the "snapshot matrix"

$$U = \begin{pmatrix} u(x_1,t_1) & u(x_1,t_2) & \dots & u(x_1,t_{N_t}) \\ u(x_2,t_1) & u(x_2,t_2) & \dots & u(x_2,t_{N_t}) \\ \vdots & \vdots & \vdots & \vdots \\ u(x_{N_x},t_1) & u(x_{N_x},t_2) & \dots & u(x_{N_x},t_{N_t}) \end{pmatrix}$$

The spatial correlation tensor of the velocity field can be set in the form :

$$R_{uu}(\mathbf{x},\mathbf{x}') = \frac{1}{N_t} U U^T$$

while the temporal correlation tensor writes :

$$R_{uu}(t,t') = \frac{1}{N_x} U^T U.$$

Stationary random processes

- Stationarity of random processes can be defined in two ways :
  - Strictly
    All the statistics of the random process are time invariant.

$$p(u_1, u_2, \dots u_N) = p(u_{1+m}, u_{2+m}, \dots u_{N+m})$$

  - Weakly
    Only one-point and two-point statistics are time invariant.

- Ergodicity
  A process is ergodic if ensemble statistics and temporal statistics match.

Proper Orthogonal Decomposition (POD)

A mathematical definition of coherent structures

G. Berkooz, P. Holmes, & J.L. Lumley, Annu. Rev. Fluid Mech. 25 (1993) 539-75

Proper orthogonal decomposition (POD) [...] has something to offer.

1. *It is statistically based-extracting data from experiments and simulations.*
2. *Its analytical foundations supply a clear understanding of its capabilities and limitations.*
3. *It permits the extraction, from a turbulent field, of spatial and temporal structures judged essential according to predetermined criteria and it provides a rigorous mathematical framework for their description.*

As such, it offers not only a tool for the analysis and synthesis of data from experiment or simulation, but also for the construction, from the Navier-Stokes equations, of low-dimensional dynamical models for the interaction of these essential structures. Thus, coming full circle, we have a statistical technique that contributes to deterministic dynamical analysis.

Coherent structures as two-point correlated events in space

The coherent structures ψ_n of the velocity field $\mathbf{u} = (u^x, u^y, u^z)$ are defined as the eigen-modes of the cross-correlation function :

$$\sum_{\alpha=1}^{n_c} \int_\Omega R_{u^\alpha u^\beta}(\mathbf{x}, \mathbf{x}') \psi_n^\alpha(\mathbf{x}') \, d\mathbf{x}' = \sigma_n \psi_n^\beta(\mathbf{x})$$

known as the Fredholm equation.
$R_{u^\alpha u^\beta}(\mathbf{x}, \mathbf{x}')$ is the two-point spatial cross-correlation tensor defined as :

$$R_{u^\alpha u^\beta}(\mathbf{x}, \mathbf{x}') = \frac{1}{T} \int_T u^\alpha(\mathbf{x}, t) u^\beta(\mathbf{x}', t) \, dt = \sum_{n=1}^{N_{POD}} \sigma_n \psi_n^\alpha(\mathbf{x}) \psi_n^{\beta\star}(\mathbf{x}')$$

- The problem is well-posed if the ψ_n are normed to 1 (constrained optimization problem)
- Eigenvectors are space dependent.
- Size : $N_{POD} = N_x \times n_c$

Classical POD or direct method (Lumley, 1967)

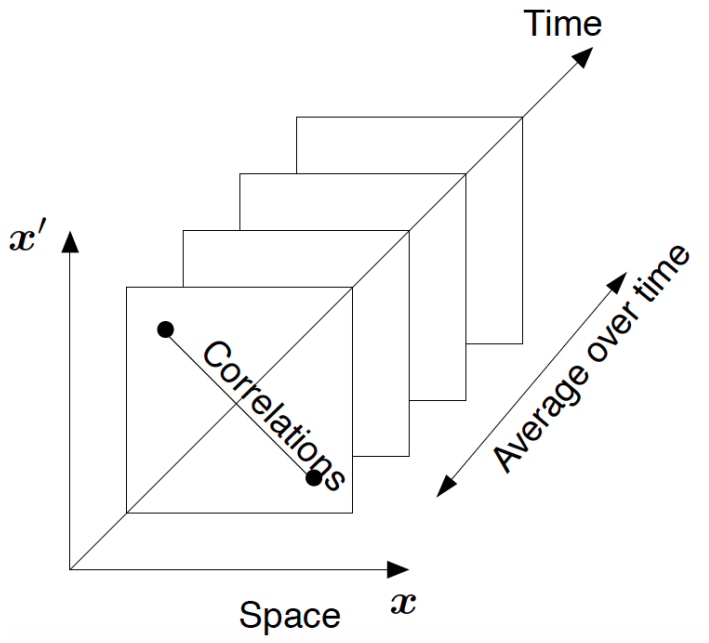

- Compute the eigenfunctions of $R_{u^\alpha u^\beta}(\mathbf{x}, \mathbf{x}')$.
- $< \cdot >_E = \frac{1}{T} \int_T \cdot \, dt$

i.e. the ensemble average is a temporal average.

Coherent structures as time correlated events ?

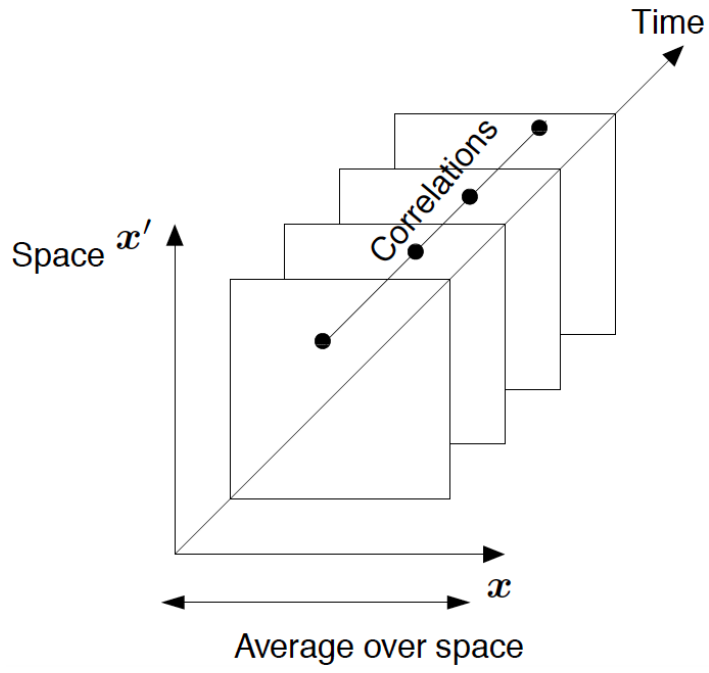

- Cannot we replace $R_{u^\alpha u^\beta}(\mathbf{x}, \mathbf{x}')$ by $R_{\mathbf{uu}}(t, t')$?
- $< \cdot >_E = \int_\Omega \cdot \, d\mathbf{x}$

  i.e. the ensemble average is a spatial average.

Snapshot POD (Sirovich, 1987)

Fredholm equation :

$$\boxed{\int_T R_{\mathbf{uu}}(t,t')\phi_n(t')\,dt' = \lambda_n \phi_n(t)}$$

where $R_{\mathbf{uu}}(t,t')$ is the two-point temporal correlation tensor defined as :

$$R_{\mathbf{uu}}(t,t') = \frac{1}{T}\int_\Omega \mathbf{u}(\mathbf{x},t)\cdot\mathbf{u}(\mathbf{x},t')\,d\mathbf{x} = \frac{1}{T}\sum_{n=1}^{N_{POD}} \sigma_n \phi_n(t)\phi_n^\star(t')$$

- Eigenvectors are time dependent.
- No cross correlations.
- Linear independence of the snapshots is assumed.
- Size : $N_{POD} = N_t$.

Recall : For the classical POD, $N_{POD} = N_x \times n_c$
$\Rightarrow$ Snapshot POD reduces drastically computational effort when $N_x \gg N_t$.

Snapshot POD or classical POD ?

What is the typical situation ?

- For experimental data : long time history with moderate spatial resolution

  $\Rightarrow$ Two-point spatial correlation tensor $R_{u^\alpha u^\beta}(\mathbf{x}, \mathbf{x}')$ well converged

  Exception : data sets obtained from Particle Image Velocimetry

- For numerical simulation data : much higher spatial resolution but a moderate time history

  $\Rightarrow$ Two-point temporal correlation tensor $R_{\mathbf{uu}}(t, t')$ well converged

- Consequences :

  - Classical POD generally used with experimental data,
  - Snapshot POD generally used with numerical data.

Common properties of the two approaches

1. Spatial modes $\boldsymbol{\psi}_n(\mathbf{x})$ are orthonormal :

$$(\boldsymbol{\psi}_n, \boldsymbol{\psi}_m) = \int_\Omega \boldsymbol{\psi}_n(\mathbf{x}) \cdot \boldsymbol{\psi}_m(\mathbf{x})\, d\mathbf{x} = \delta_{nm}.$$

2. Each space-time realization $\mathbf{u}(\mathbf{x}, t)$ can be expanded into the basis of the orthogonal eigen-modes $\boldsymbol{\psi}_n(\mathbf{x})$ with uncorrelated coefficients $\phi_n(t)$:

$$\mathbf{u}(\mathbf{x}, t) = \sum_{n=1}^{N_{POD}} \sigma_n \phi_n(t) \boldsymbol{\psi}_n(\mathbf{x}),$$

   where σ_n accounts for the fraction of kinetic energy extracted by $\boldsymbol{\psi}_n(\mathbf{x})$ from the snapshot set of the velocity field.

3. The time coefficients $\phi_n(t)$ are orthogonal :

$$\frac{1}{T} \int_T \phi_n(t) \phi_m^\star(t)\, dt = \delta_{nm}.$$

POD Important consequences

- The spatial basis functions $\boldsymbol{\psi}_n(\mathbf{x})$ can be estimated as :

$$\boldsymbol{\psi}_n(\mathbf{x}) = \frac{1}{T\lambda_n} \int_T \mathbf{u}(\mathbf{x}, t)\phi_n^\star(t)\, dt$$

  i.e. as a linear combination of the instantaneous velocity fields.

  $\Rightarrow$ The $\boldsymbol{\psi}_n(\mathbf{x})$ possess all the properties of $\mathbf{u}(\mathbf{x}, t)$ that can be written as linear and homogeneous equations.

- For an incompressible flow

$$\nabla \cdot \mathbf{u} = 0 \quad \Rightarrow \quad \nabla \cdot \boldsymbol{\psi}_n = 0 \quad \forall n = 1, \ldots, N_{POD}$$

- Same boundary conditions

  If they are homogeneous, then they are satisfied by each of the eigenfunctions individually.

POD : different approaches

POD approaches depend on :

- the inner product :
  - L^2
  - H^1
  - ...
- the kind of correlations :
  - spatial $x = (x, y, z)$
  - temporal t
  - control parameters c, for instance Reynolds number . . .
- the ensemble average $< \cdot >_E$
  - spatial
  - temporal

Other names

- Also known as :
  - Karhunen-Loève decomposition : Karhunen (1946), Loève (1945) ;
  - Principal Component Analysis : Hotelling (1953) ;
  - Singular Value Decomposition : Golub and Van Loan (1983).
- Applications include :
  - Random variables (Papoulis, 1965) ;
  - Image processing (Rosenfeld and Kak, 1982) ;
  - Signal analysis (Algazi and Sakrison, 1969) ;
  - Data compression (Andrews, Davies and Schwartz, 1967) ;
  - Process identification and control (Gay and Ray, 1986) ;
  - Optimal control (Ravindran, 2000 ; Hinze et Volkwein 2004 ; Bergmann, 2004) and of course in fluid mechanics
- Introduced in turbulence by Lumley (1967)

  Lumley J.L. (1967) : The structure of inhomogeneous turbulence. Atmospheric Turbulence and Wave Propagation, ed. A.M. Yaglom & V.I. Tatarski, pp. 166-178.

Choice of inner product and associated norm

1. L^2 inner product (the most used)

$$L^2 = \{\text{square integrable functions}\}$$

$$(\mathbf{u}, \mathbf{v}) = \sum_{\Omega} (u_1 v_1^\star + u_2 v_2^\star + u_3 v_3^\star)\, d\mathbf{x} \quad ; \quad \|\mathbf{u}\|^2 = (\mathbf{u}, \mathbf{u}) \quad ; \quad E_c = \frac{1}{2}\rho \|\mathbf{u}\|^2$$

$\Rightarrow L^2$ is a natural space in which to do fluid mechanics since it corresponds to flows having finite kinetic energy.

2. H^1 inner product (Iollo et al., 2000)

$$H^1(\Omega) = \{u \in L^2(\Omega) : \frac{\partial u}{\partial x_i} \in L^2(\Omega)\} : \text{ Sobolev space}$$

$$(u, v) = \int_\Omega (u, v) d\mathbf{x} + \varepsilon \int_\Omega (\nabla u \cdot \nabla v) d\mathbf{x}$$

where ε is a parameter.

Choice of inner product and associate norm

3. Inner product for aeroacoustic compressible flow (Rowley et al., 2001)

Flow variables $\mathbf{q} = (u, v, a)$ where u and v are the 2D velocities and a is the local sound speed :

$$(\mathbf{q}_1, \mathbf{q}_2)_\varepsilon = \int_\Omega \left(u_1 u_2 + v_1 v_2 + \frac{2\varepsilon}{\gamma(\gamma-1)} a_1 a_2 \right) d\mathbf{x}$$

where γ is the ratio of specific heats and ε is a parameter.

- if $\varepsilon = \gamma$ then $\|q\|^2 = 2h_0$ i.e. twice the total enthalpy of the flow,
- if $\varepsilon = 1$ then $\|q\|^2$ gives twice the total energy of the flow.

Snapshot Data Matrix

$$\mathbf{u} = (u, v, w) \quad ; \quad \mathbf{x} \in \{x_1, x_2, \ldots, x_{N_x}\} \quad ; \quad t \in \{t_1, t_2, \ldots, t_{N_t}\}$$

$$A = \left(\begin{array}{c|c|c|c|c}
u(x_1,t_1) & u(x_1,t_2) & \ldots & u(x_1,t_{N_t-1}) & u(x_1,t_{N_t}) \\
v(x_1,t_1) & v(x_1,t_2) & \ldots & v(x_1,t_{N_t-1}) & v(x_1,t_{N_t}) \\
w(x_1,t_1) & w(x_1,t_2) & \ldots & w(x_1,t_{N_t-1}) & w(x_1,t_{N_t}) \\
\hline
u(x_2,t_1) & u(x_2,t_2) & \ldots & u(x_2,t_{N_t-1}) & u(x_2,t_{N_t}) \\
v(x_2,t_1) & v(x_2,t_2) & \ldots & v(x_2,t_{N_t-1}) & v(x_2,t_{N_t}) \\
w(x_2,t_1) & w(x_2,t_2) & \ldots & w(x_2,t_{N_t-1}) & w(x_2,t_{N_t}) \\
\hline
\vdots & \vdots & \vdots & \vdots & \vdots \\
\hline
u(x_{N_x},t_1) & u(x_{N_x},t_2) & \ldots & u(x_{N_x},t_{N_t-1}) & u(x_{N_x},t_{N_t}) \\
v(x_{N_x},t_1) & v(x_{N_x},t_2) & \ldots & v(x_{N_x},t_{N_t-1}) & v(x_{N_x},t_{N_t}) \\
w(x_{N_x},t_1) & w(x_{N_x},t_2) & \ldots & w(x_{N_x},t_{N_t-1}) & w(x_{N_x},t_{N_t})
\end{array}\right)$$

with $A \in \mathbb{R}^{(3N_x)\times N_t}$.

Singular Value Decomposition (SVD)

$$A = \Psi \Sigma \Phi^T \quad \in \quad \mathbb{R}^{3N_x \times N_t}$$

where

$$\Psi \in \mathbb{R}^{3N_x \times 3N_x} \quad ; \quad \Sigma \in \mathbb{R}^{3N_x \times N_t} \quad ; \quad \Phi \in \mathbb{R}^{N_t \times N_t}$$

- Left singular vectors : $\Psi = (\psi_1, \psi_2, \ldots, \psi_{3N_x}), \Psi\Psi^T = I_{3N_x}$
- Right singular vectors : $\Phi = (\phi_1, \phi_2, \ldots, \phi_{N_t}), \Phi\Phi^T = I_{N_t}$
- Singular values : $\sigma_i, i = 1, \ldots, p = \min(3N_x, N_t)$

$$\Sigma = \mathrm{diag}(\sigma_1, \ldots, \sigma_p, 0 \ldots, 0) \quad \text{with}$$

$\sigma_1 \geq \sigma_2 \geq \ldots \geq \sigma_r > \sigma_{r+1} = \sigma_{r+2} = \ldots = \sigma_p = 0$ where $r = \mathrm{rank}(A) \leq p$.

- SVD and eigenvalue problems
  - $AA^T = \Psi\Sigma^2\Psi^T = \Psi\Lambda\Psi^T$ with $AA^T \in \mathbb{R}^{3N_x \times 3N_x}$
  - $A^TA = \Phi\Sigma^2\Phi^T = \Phi\Lambda\Phi^T$ with $A^TA \in \mathbb{R}^{N_t \times N_t}$

$$\Rightarrow \sigma_i = \sqrt{\lambda_i(AA^T)} = \sqrt{\lambda_i(A^TA)}$$

SVD for $3N_x < N_t$

For $3N_x < N_t$, $A = \Psi\Sigma\Phi^T \in \mathbb{R}^{3N_x \times N_t}$ writes :

$$A = \begin{pmatrix} \psi_1 & \dots & \psi_{3N_x} \end{pmatrix} \left(\begin{array}{ccc|ccc} \sigma_1 & & & 0 & \dots & 0 \\ & \ddots & & \vdots & & \vdots \\ & & \ddots & \vdots & & \vdots \\ & & & \vdots & & \vdots \\ & & \sigma_{3N_x} & 0 & \dots & 0 \end{array}\right) \left(\begin{array}{c} \phi_1^T \\ \vdots \\ \vdots \\ \phi_{3N_x}^T \\ \hline \phi_{3N_x+1}^T \\ \vdots \\ \vdots \\ \phi_{N_t}^T \end{array}\right)$$

SVD for $3N_x > N_t$

For $3N_x > N_t$, $A = \Psi\Sigma\Phi^T \in \mathbb{R}^{3N_x \times N_t}$ writes :

$$A = \begin{pmatrix} \psi_1 & \dots & \psi_{N_t} & \psi_{N_t+1} & \dots & \psi_{3N_x} \end{pmatrix} \begin{pmatrix} \sigma_1 & & & & \\ & \ddots & & & \\ & & \ddots & & \\ & & & \ddots & \\ & & & & \sigma_{N_t} \\ \hline 0 & \dots & \dots & \dots & 0 \\ \vdots & & & & \vdots \\ \vdots & & & & \vdots \\ 0 & \dots & \dots & \dots & 0 \end{pmatrix} \begin{pmatrix} \phi_1^T \\ \vdots \\ \vdots \\ \vdots \\ \vdots \\ \vdots \\ \vdots \\ \phi_{N_t}^T \end{pmatrix}$$

SVD Dyadic decomposition and norms

- Dyadic decomposition :

$$
\begin{aligned}
A_{3N_x \times N_t} &= \Psi_{3N_x \times 3N_x} \Sigma_{3N_x \times N_t} \Phi^T_{N_t \times N_t} \\
&= \begin{pmatrix} \underline{\Psi}_{3N_x \times r} & \bar{\Psi}_{3N_x \times (N_t - r)} \end{pmatrix} \begin{pmatrix} \Sigma_{r \times r} & 0 \\ 0 & 0 \end{pmatrix} \begin{pmatrix} \underline{\Phi}_{N_t \times r} & \bar{\Phi}_{N_t \times (N_t - r)} \end{pmatrix}^T \\
&= \Psi_{3N_x \times r} \Sigma_{r \times r} \Phi^T_{N_t \times r}
\end{aligned}
$$

$$
\boxed{A_{3N_x \times N_t} = \sigma_1 \psi_1 \phi_1^T + \sigma_2 \psi_2 \phi_2^T + \ldots + \sigma_r \psi_r \phi_r^T .}
$$

- 2-induced norm $\|A\|_2 = \max_{\|\mathbf{v}\|_2 = 1} \|A\mathbf{v}\|_2 = \sigma_1$.

- Frobenius norm $\|A\|_F = \sum_{i=1}^{3N_x} \sum_{j=1}^{N_t} a_{ij}^2 = \sqrt{\sum_{i=1}^{r} \sigma_i^2}$

Low rank approximation of A

Let $A \in \mathbb{R}^{3N_x \times N_t}$.

Determine $A_k \in \mathbb{R}^{3N_x \times N_t}$ such that $\mathrm{rank}(A_k) = k < \mathrm{rank}(A)$ which minimizes the 2-norm (or Frobenius norm) of the error $E = A - A_k$.

Eckart-Young theorem :

$$\min_{\mathrm{rank}(A_k) \leq k} \|A - A_k\|_2 = \sigma_{k+1}(A)$$

$$\min_{\mathrm{rank}(A_k) \leq k} \|A - A_k\|_F = \sqrt{\sum_{i=k+1}^{r} \sigma_i^2(A)}$$

$$\text{with } A_k = \Psi \begin{pmatrix} \Sigma_k & 0 \\ 0 & 0 \end{pmatrix} \Phi^T = \sigma_1 \psi_1 \phi_1^T + \sigma_2 \psi_2 \phi_2^T + \ldots + \sigma_k \psi_k \phi_k^T$$

Remark : This theorem establishes a relationship between the rank k of the approximant, and the singular values of A.

Image compression by truncated SVD Generalities

- Consider an image with $n_x \times n_y$ pixels. This image can be stored as a matrix $A \in \mathbb{R}^{n_x \times n_y}$ where a_{ij} contains the grey level of pixel (i, j).
- Memory $n_x \times n_y$ bytes + header
- Eckart-Young th. : best approximation of A with rank r writes

$$\hat{A} = \sigma_1 \psi_1 \phi_1^T + \sigma_2 \psi_2 \phi_2^T + \ldots + \sigma_r \psi_r \phi_r^T,$$

and is such that

$$\|A - \hat{A}\|_2 = \sigma_{r+1}.$$

- Size reduction
  - Store $\psi_1, \ldots, \psi_r, \sigma_1 \phi_1^T, \ldots, \sigma_r \phi_r^T$ in place of A
  - Memory $r \times (n_x + n_y)$ bytes.

$\Rightarrow$ Interesting method if r is low.

Image compression by truncated SVD clown & trees

Clown : matrix 200×330
rank : 200, size : 258 kb

Trees : matrix 128×128
rank : 128, size : 64 kb

Image compression by truncated SVD singular values

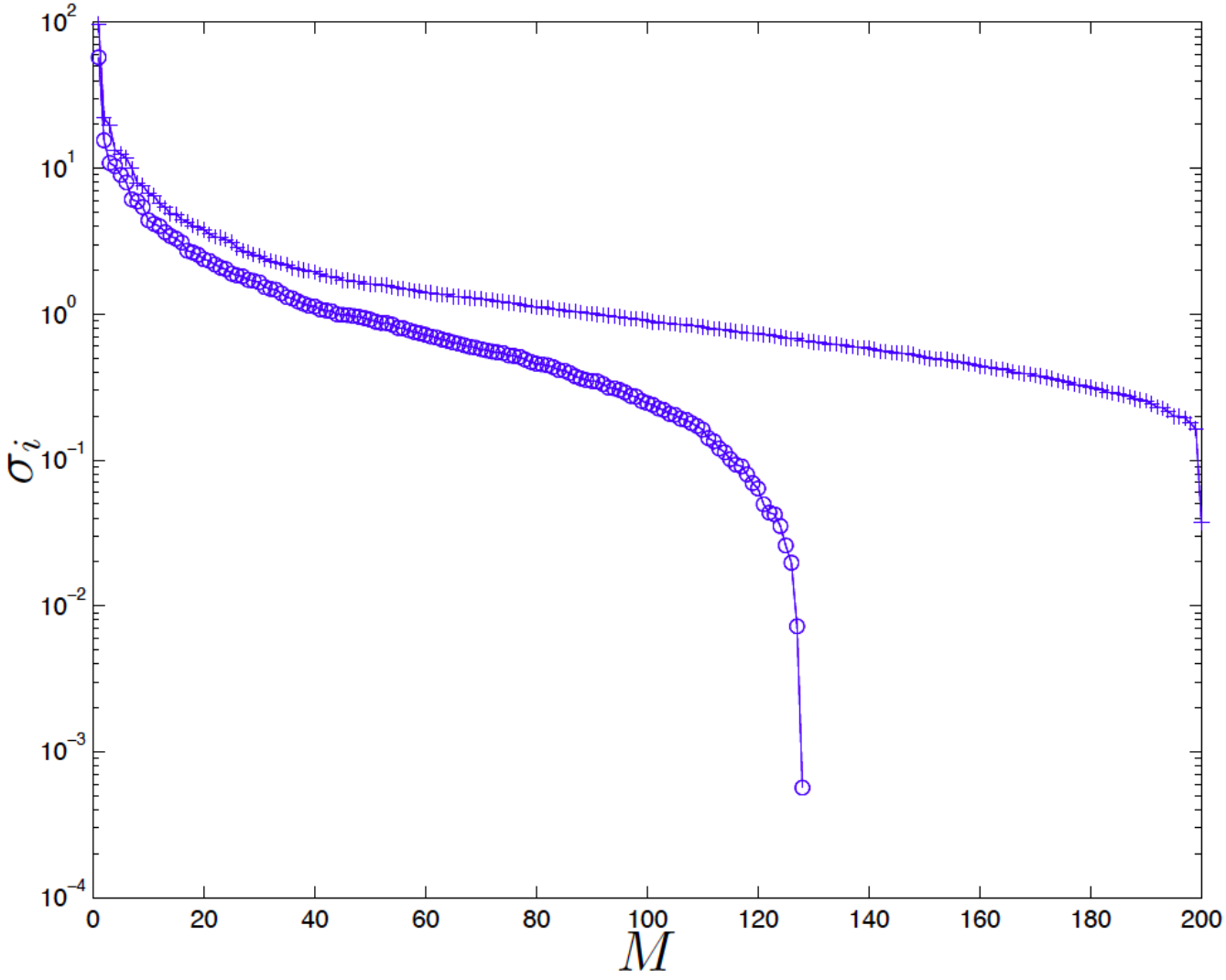

$+$: "clown" image ; $\circ$: "trees" image

Relative Information Content (RIC)

For an image of rank r :

$$RIC(M) = \frac{\sum_{i=1}^{M \geq r} \sigma_i}{\sum_{i=1}^{r} \sigma_i}$$

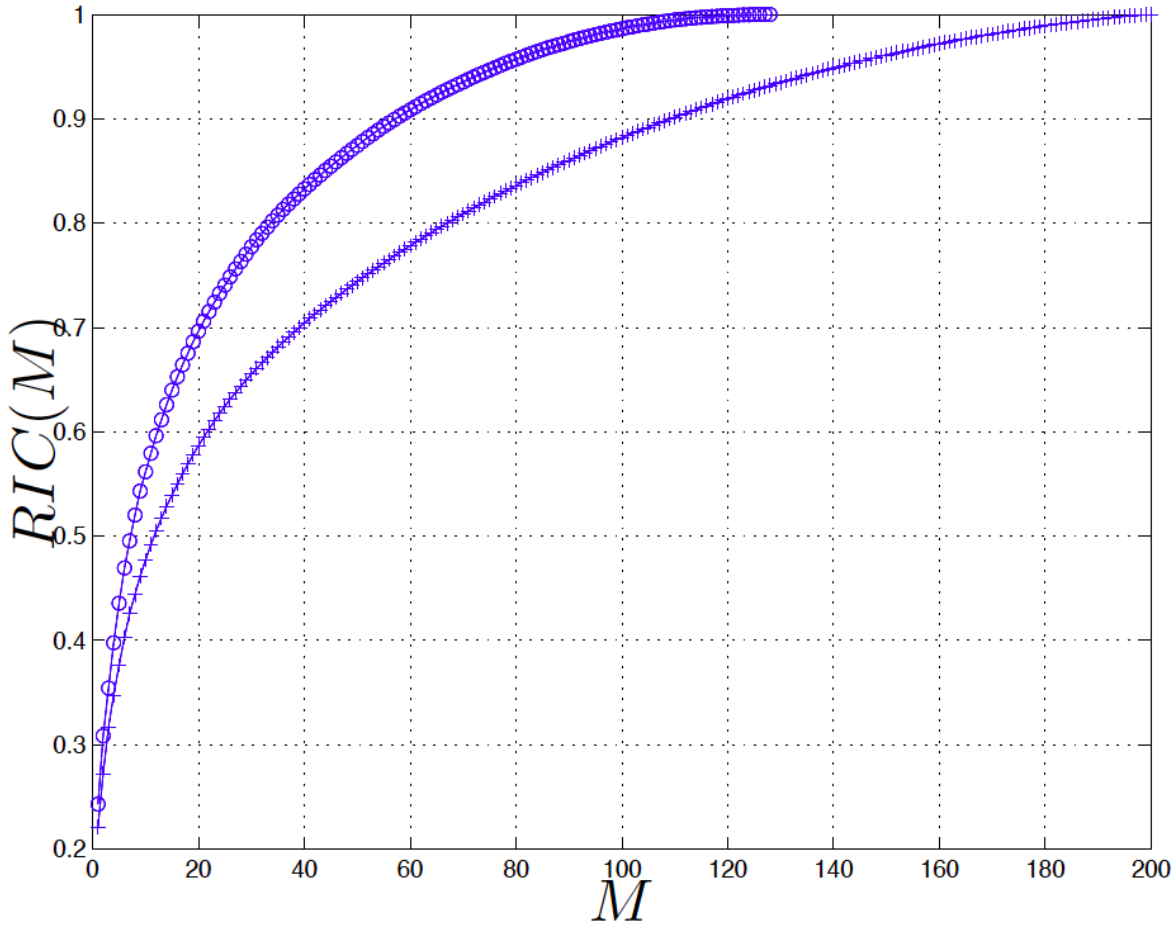

Image compression by truncated SVD "clown"

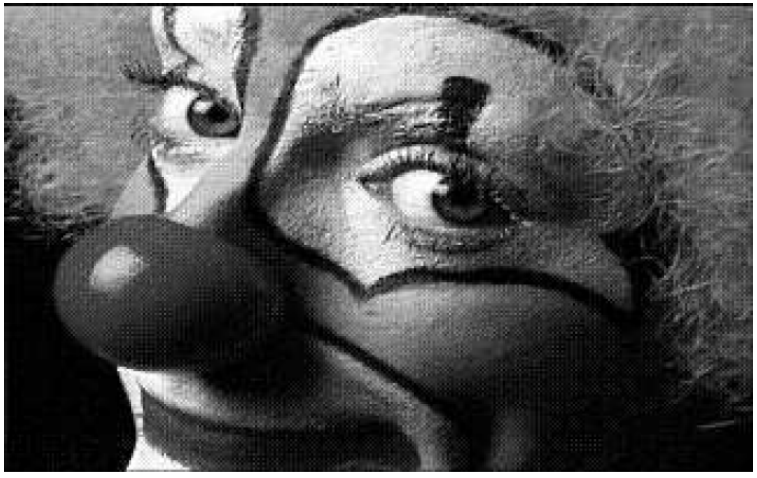

Original image ; size : 258 kb

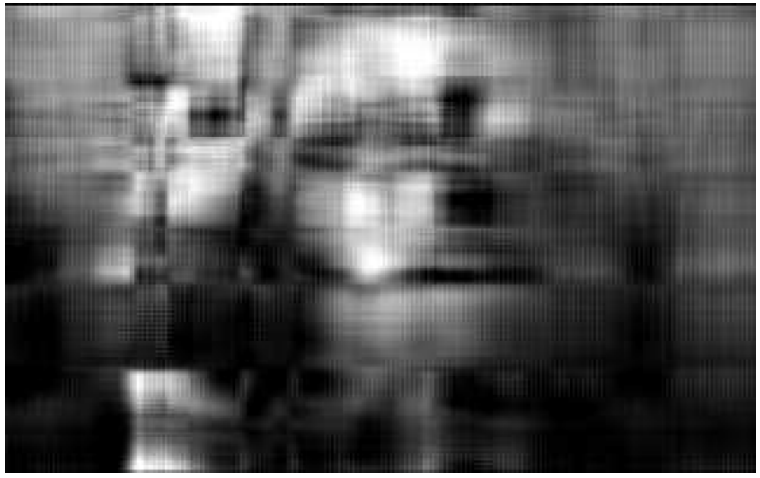

App. of rank 6 ; size : 12,4 kb
Reduction : 95.2%

App. of rank 12 ; size : 24,8 kb
Reduction : 90.4%

App. of rank 20 ; size : 41,4 kb ;
Reduction : 84%

Image compression by truncated SVD "trees"

Original image ; size : 64 kb

App. of rank 6 ; size : 6 kb
Reduction : 90.6%

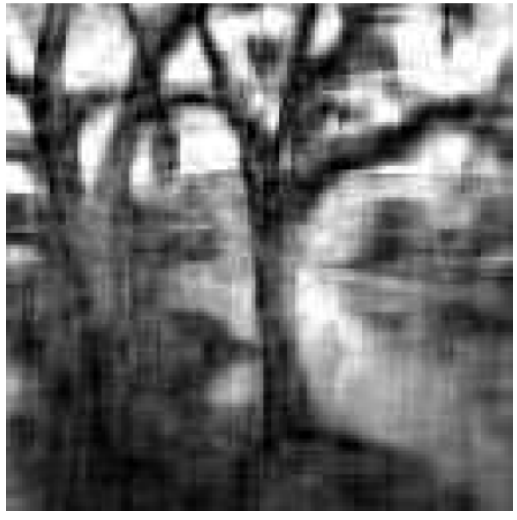

App. of rank 12 ; size : 12 kb
Reduction : 81.2%

App. of rank 20 ; size : 20 kb
Reduction : 68.8%

POD applied to the cylinder wake flow

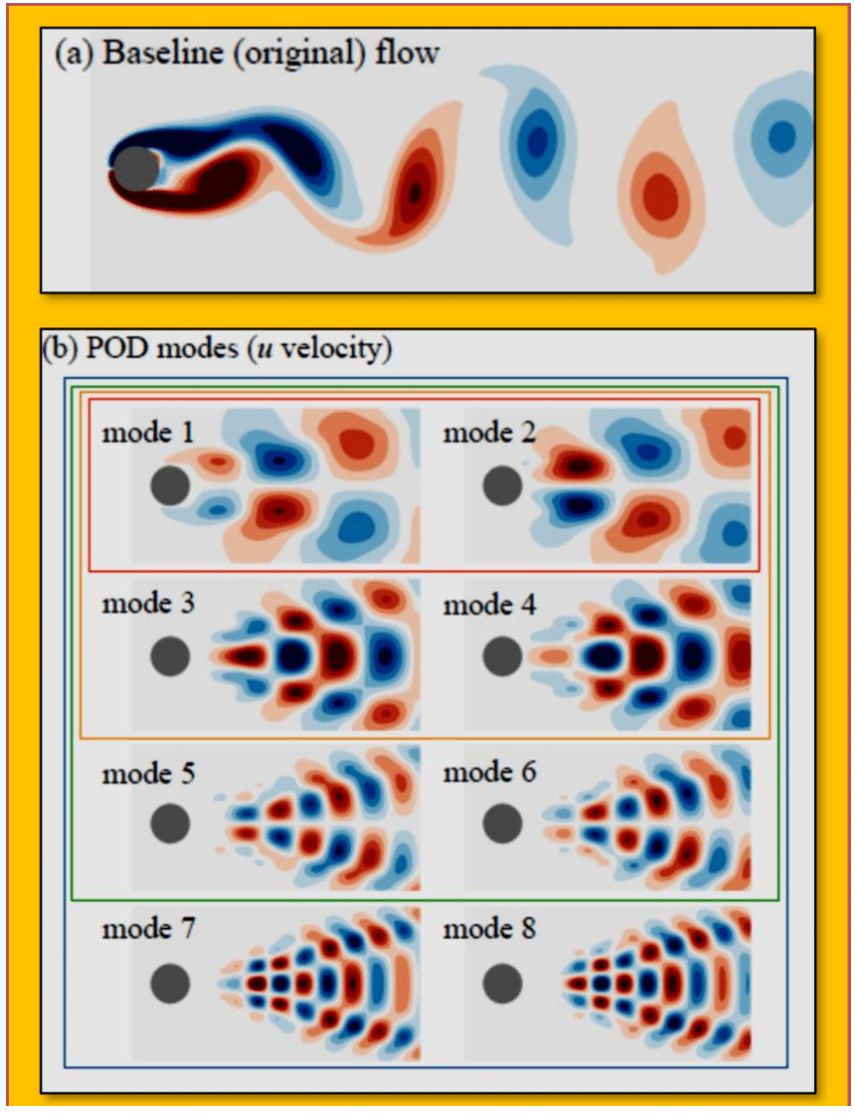

Idreen Sadrehaghighi's courtesy

POD applied to the 3D cylinder wake flow

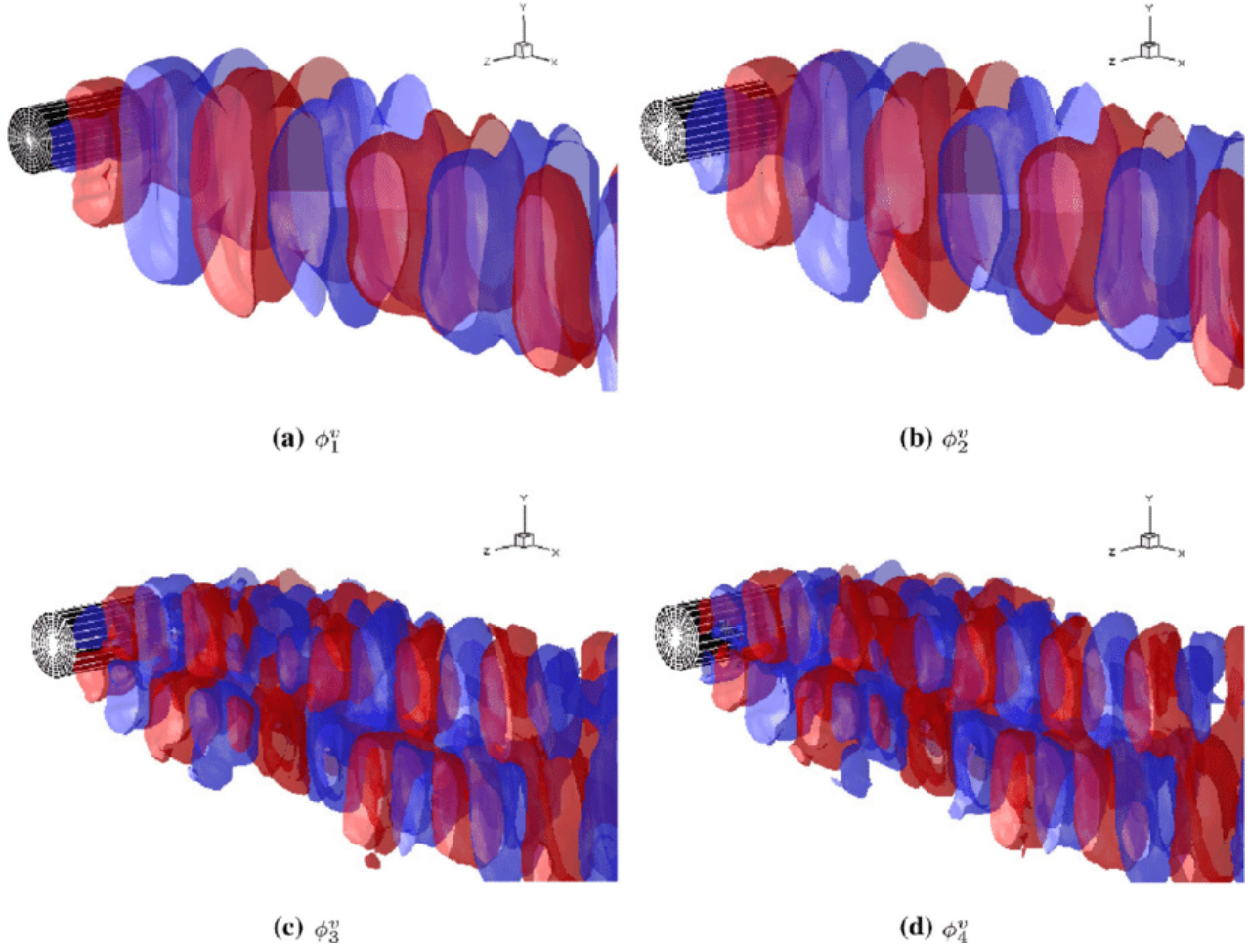

(a) ϕ_1^v (b) ϕ_2^v (c) ϕ_3^v (d) ϕ_4^v

Akhtar Imran's courtesy

POD modes of the cavity flow

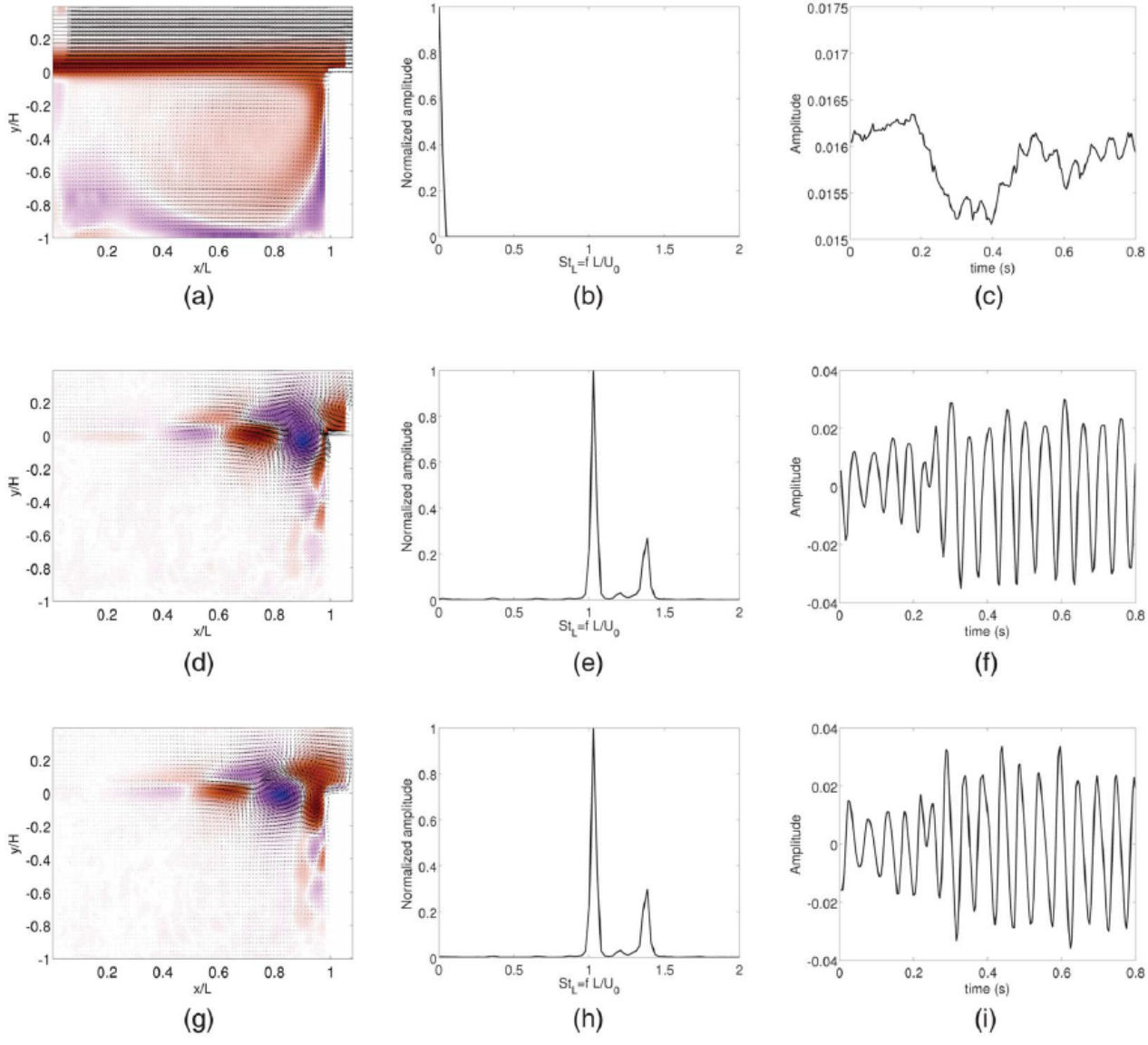

POD modes of the cavity flow

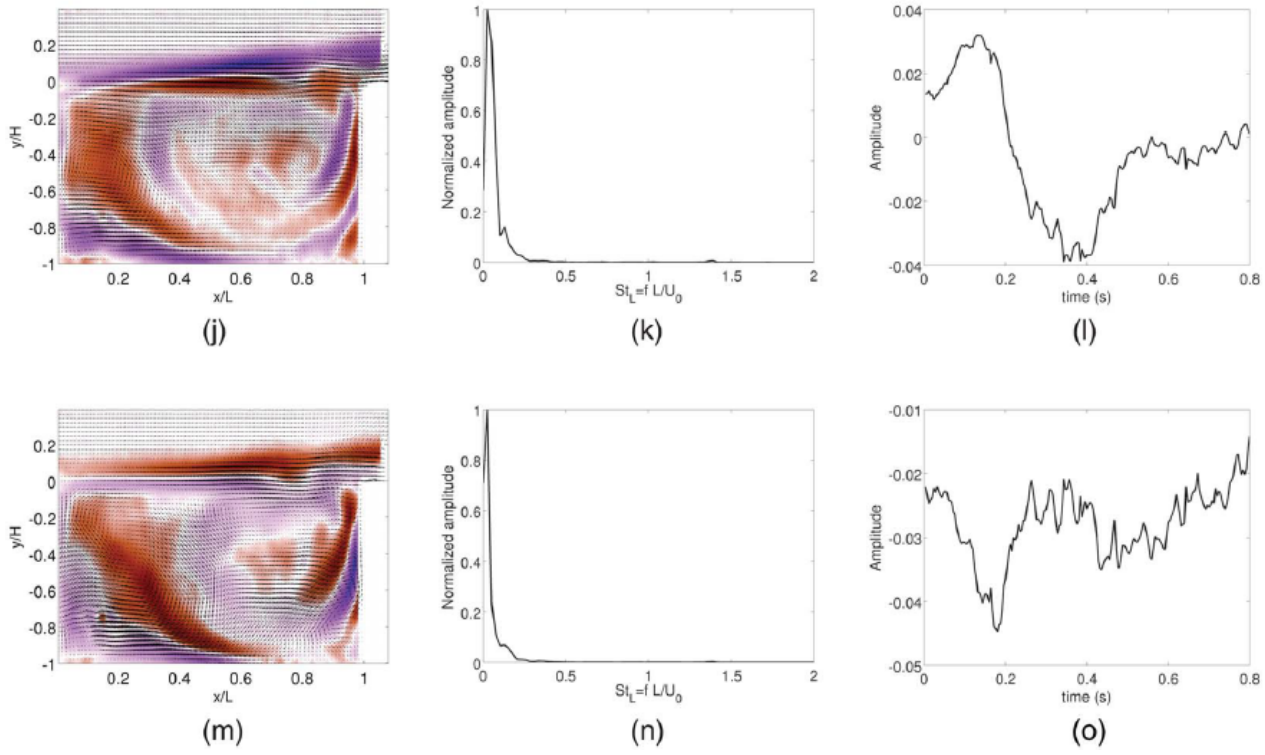

from F. Guéniat, L. Pastur, F. Lusseyran, Physics of Fluids 26 (2014) 085101

POD : pro & cons

- Pros
  - POD provides a mathematical definition of coherent structures.
  - POD is an energy-based decomposition of the flow field : it is optimal and robust with respect to energy.
  - The POD modes form a complete basis for data set.
- Cons.
  - Possible spectral mixing.
  - Localized travelling patterns require several POD modes for a proper description.

Dynamic Mode Decomposition (DMD)

What is DMD aimed at ?

P.J. Schmid, JFM (2010) :

> *The description of coherent features of fluid flow is essential to our understanding of fluid-dynamical and transport processes. A method is introduced that is able to extract dynamic information from flow fields that are either generated by a (direct) numerical simulation or visualized/measured in a physical experiment. The extracted* **dynamic modes**, *which can be interpreted as a generalization of global stability modes, can be used to describe the underlying physical mechanisms captured in the data sequence or to project large-scale problems onto a dynamical system of significantly fewer degrees of freedom.*

What is DMD aimed at ?

C. Rowley et al, JFM (2009) :

> *The global behaviour of complex nonlinear flows is described by decomposing the flow into modes determined from spectral analysis of the Koopman operator, an infinite-dimensional linear operator associated with the full nonlinear system. The* **Koopman modes** *are associated with a particular observable, and may be determined directly from data (either numerical or experimental) using a variant of a standard Arnoldi method. They have an associated temporal frequency and growth rate and may be viewed as a nonlinear generalization of global eigenmodes of a linearized system. They provide an alternative to proper orthogonal decomposition, and in the case of periodic data the Koopman modes reduce to a discrete temporal Fourier transform.*

The Koopman operator

Consider a dynamical system evolving on a manifold M such that, for the state vector $\mathbf{X}_k \in M$ at time t_k

$$\mathbf{X}_{k+1} = \mathbf{f}(\mathbf{X}_k),$$

where $\mathbf{f} : M \to M$.

The **Koopman operator** K is a linear operator that maps any scalar-valued function $g : M \to \mathbb{R}^m$ into a new function Kg as

$$Kg(\mathbf{X}) = g(\mathbf{f}(\mathbf{X})).$$

A linear operator

K is a linear operator :

$$K(\alpha g_1 + \beta g_2)(\mathbf{X}) = \alpha K g_1(\mathbf{X}) + \beta K g_2(\mathbf{X})$$

for any functions g_1, g_2 and scalars α, β.

Important remark :

Although the dynamical system is *nonlinear* and evolves on a *finite-dimensional* manifold M, the Koopman operator K is *linear infinite dimensional*.

A data-driven analysis

Let $\varphi_j : M \to \mathbb{C}$ denote eigenfunctions and $\lambda_j \in \mathbb{C}$ eigenvalues of the Koopman operator :

$$K\varphi_j(\mathbf{X}) = \lambda_j \varphi_j(\mathbf{X}), \qquad j = 1, 2, \ldots$$

Consider that $\mathbf{X} \in M$ contains the full information about the flow field at a particular time (state vector).

$\mathbf{g}(\mathbf{X}) : M \to \mathbb{R}^m$ is a vector of any quantities of interest, such as a velocity measurements at various points in the flow.

If each of the m components of $\mathbf{g}$ lies within the span of the eigenfunctions $\{\varphi_j\}$, then we may expand the vector-valued $\mathbf{g}$ in terms of these eigenfunctions as

$$\mathbf{g}(\mathbf{X}) = \sum_{j \geq 1} \varphi_j(\mathbf{X}) \boldsymbol{\xi}_j.$$

The eigenfunctions φ_j are referred to as the Koopman eigenfunctions, the corresponding vectors $\boldsymbol{\xi}_j$ as the Koopman modes of the *map* $\mathbf{f}$ corresponding to the *observable* $\mathbf{g}$.

Discrete time evolution

Iterates of $\mathbf{X}_0$ are given by

$$\mathbf{g}(\mathbf{X}_k) = \sum_{j \geq 1} K^k \varphi_j(\mathbf{X}_0) \boldsymbol{\xi}_j = \sum_{j=1} \lambda_j^k \varphi_j(\mathbf{X}_0) \boldsymbol{\xi}_j.$$

The Koopman eigenvalues $\lambda_j \in \mathbb{C}$ characterize the temporal behaviour of the corresponding Koopman mode $\boldsymbol{\xi}_j$:

- the phase of λ_j determines the angular frequency : $\omega_j = \Im \log(\lambda_j)/\Delta t$
- the magnitude of λ_j determines the growth rate : $\sigma_j = \Re \log(\lambda_j)/\Delta t$

Remark :

If the components of $\mathbf{g}$ do not lie within the span of the eigenfunctions of K, one may split K into regular and singular components, and project components of $\mathbf{g}$ onto the span of the eigenfunctions

Koopman modes for linear systems

Suppose M is a n-dimensional linear space, and suppose the map $\mathbf{f}$ is linear :

$$\mathbf{f}(\mathbf{X}) = \mathbf{A}\mathbf{X}.$$

Let $\boldsymbol{\xi}_j$ and λ_j be eigenvectors and eigenvalues of $\mathbf{A}$: $\mathbf{A}\boldsymbol{\xi}_j = \lambda_j \boldsymbol{\xi}_j$,
Let $\mathbf{w}_j$ be the corresponding eigenfunctions of the adjoint $\mathbf{A}^\star$: $\mathbf{A}^\star \mathbf{w}_j = \bar{\lambda}_j \mathbf{w}_j$,
normalized so that $< \boldsymbol{\xi}_j, \mathbf{w}_k >= \delta_{jk}, \quad _{j,k=1,\ldots,n}$.

The scalar-valued functions $\varphi_j(\mathbf{X}) =< \mathbf{X}, \mathbf{w}_j >$, $j = 1, \ldots, n$, are eigenfunctions of K with eigenvalues λ_j. Indeed :

$$K\varphi_j(\mathbf{X}) = \varphi_j(\mathbf{A}\mathbf{X}) =< \mathbf{A}\mathbf{X}, \mathbf{w}_j >=< \mathbf{X}, \mathbf{A}^\star \mathbf{w}_j >= \lambda_j < \mathbf{X}, \mathbf{w}_j >= \lambda_j \varphi_j(\mathbf{X}).$$

Now, for any $\mathbf{X} \in M$, as long as $\mathbf{A}$ has a full set of eigenvectors, we may write

$$\mathbf{X} = \sum_{j=1}^{n} < \mathbf{X}, \mathbf{w}_j > \boldsymbol{\xi}_j = \sum_{j=1}^{n} \lambda_j \varphi_j(\mathbf{X}) \boldsymbol{\xi}_j.$$

$\Rightarrow$ For linear systems, the Koopman modes coincide with the eigenvectors of $\mathbf{A}$.

Remark : Unlike $\mathbf{A}$, the operator K has a countably infinite number of eigenvalues, since λ_j^k is also an eigenvalue, with eigenfunction $\varphi_j(\mathbf{X})^k$, for any integer k.

Koopman modes for periodic solutions

Suppose that the set of distinct vectors $S = \{\mathbf{X}_0, \ldots, \mathbf{X}_{n-1}\}$ forms a periodic solution of the system :

$$\mathbf{X}_{k+n} = \mathbf{X}_k \quad \text{for all } k.$$

Define the new set of vectors $\{\hat{\mathbf{X}}_0, \ldots, \hat{\mathbf{X}}_{n-1}\}$ by applying the discrete Fourier transform to $\mathbf{X}$:

$$\mathbf{X}_k = \sum_{j=0}^{n-1} \exp\left(2\pi \mathrm{i} jk/n\right) \hat{\mathbf{X}}_j, \quad k = 0, \ldots, n-1.$$

Define the set of functions $\varphi_j : S \to \mathbb{C}$ by $\varphi_j(\mathbf{X}_k) = \exp\left(2\pi \mathrm{i} jk/n\right)$,$j,k=0,\ldots,n-1$.
The φ_j are eigenfunctions of the Koopman operator K with eigenvalues $\exp\left(2\pi \mathrm{i} j/n\right)$:

$$K\varphi_j(\mathbf{X}_k) = \varphi_j(\mathbf{f}(\mathbf{X}_k)) = \varphi_j(\mathbf{X}_{k+1}) = \exp\left(2\pi \mathrm{i} j(k+1)/n\right) = \exp\left(2\pi \mathrm{i} j/n\right) \varphi_j(\mathbf{X}_k).$$

Therefore,

$$\mathbf{X}_k = \sum_{j=0}^{n-1} \varphi_j(\mathbf{X}_k) \hat{\mathbf{X}}_j.$$

→ The Koopman modes are the vectors $\hat{\mathbf{X}}_j$

→ The phase of the corresponding eigenvalues are the frequencies j/n.

Koopman operator on attractors

When the dynamics is non-periodic but evolves on an attractor, the following properties hold :

- The Koopman eigenvalues lie on the unit circle.
- The Koopman modes may be calculated by harmonic averages, which for finite-time datasets reduce to discrete Fourier transforms.

Dynamic modes vs Koopman modes

DMD provides an approximation of the action of the Koopman operator on a finite-dimensional (Krylov) subspace spanned by (time-resolved) realizations of the velocity field.

Application to snapshots of the velocity field

- Input :
  Consider an ensemble of snapshots $\mathbf{v}_i$, $i = 1, \cdots, N$ such that

$$V_1^N = \{\mathbf{v}_1, \mathbf{v}_2, \mathbf{v}_3, \cdots, \mathbf{v}_N\} \in \mathbb{R}^{m \times N}$$

- Hypothesis #1 :
  Assume a linear mapping A between $\mathbf{v}_i$ and $\mathbf{v}_{i+1}$

$$\mathbf{v}_{i+1} = A\mathbf{v}_i \quad \text{with} \quad A \in \mathbb{R}^{m \times m}$$

  i.e. V_1^N is Krylov matrix of dimension $m \times N$

$$V_1^N = \left\{\mathbf{v}_1, A\mathbf{v}_1, A^2\mathbf{v}_1, \cdots, A^{N-1}\mathbf{v}_1\right\}$$

- Objective : Determine a good approximation of the eigen-elements of A — without knowing A !

The Companion matrix

- Hypothesis #2 :
  If N is sufficiently large, we can express $\mathbf{v}_N$ as a linear combination of the previous $\mathbf{v}_i$, $(i = 1, \cdots, N-1)$ *i.e.*

$$\begin{aligned}\mathbf{v}_N &= c_1\mathbf{v}_1 + c_2\mathbf{v}_2 + \cdots + c_{N-1}\mathbf{v}_{N-1} + \mathbf{r} \\ &= V_1^{N-1}\mathbf{c} + \mathbf{r}\end{aligned}$$

  where $\mathbf{r} \in \mathbb{R}^m$ and $\mathbf{c} = (c_1, c_1, \cdots, c_{N-1})^T \in \mathbb{R}^{N-1}$

- Ruhe (1984) proved that

$$\boxed{AV_1^{N-1} = V_1^{N-1}S + \mathbf{r}\mathbf{e_{N-1}}^T} \tag{1}$$

  where $\mathbf{e_i}$ is the ith Euclidean unitary vector of length $(N-1)$ and S a Companion matrix

$$S = \begin{pmatrix} 0 & 0 & \dots & 0 & c_1 \\ 1 & 0 & \dots & 0 & c_2 \\ 0 & 1 & \dots & 0 & c_3 \\ \vdots & \vdots & \vdots & \vdots & \vdots \\ 0 & 0 & \dots & 1 & c_{N-1} \end{pmatrix} \in \mathbb{R}^{(N-1)\times(N-1)}$$

Ritz eigenvalues

- If we already know eigen-elements of S then we can determine approximated eigen-elements of A. Indeed, we can demonstrate that :

$$\boxed{\text{if} \quad S\mathbf{y_i} = \mu_i \mathbf{y_i} \qquad \text{then} \qquad A\mathbf{z_i} \simeq \mu_i \mathbf{z_i} \quad \text{with} \quad \mathbf{z_i} = V_1^{N-1}\mathbf{y_i}}$$

Proof :

$$\begin{aligned} A\mathbf{z_i} - \mu_i \mathbf{z_i} &= AV_1^{N-1}\mathbf{y_i} - \mu_i V_1^{N-1}\mathbf{y_i} \\ &= AV_1^{N-1}\mathbf{y_i} - V_1^{N-1}S\mathbf{y_i} \\ &= \left(AV_1^{N-1} - V_1^{N-1}S\right)\mathbf{y_i} = \mathbf{r}\mathbf{e_{N-1}}^T\mathbf{y_i} \longrightarrow 0 \quad \text{if} \quad \|\mathbf{r}\| \longrightarrow 0 \end{aligned}$$

The Vandermonde matrix

When the eigenvalues are distinct, the diagonalisation of $C = Y^{-1}\Lambda Y$ involves a **Vandermonde** matrix :

$$Y = \begin{pmatrix} 1 & \mu_1 & \mu_1^2 & \dots & \mu_1^{N-2} \\ 1 & \mu_2 & \mu_2^2 & \dots & \mu_2^{N-2} \\ \vdots & \vdots & \vdots & \vdots & \\ 1 & \mu_{N-1} & \mu_{N-1}^2 & \dots & \mu_{N-1}^{N-2} \end{pmatrix} \qquad \text{where } \Lambda = \operatorname{diag}(\mu_1, \dots, \mu_{N-1}).$$

If now $\mathbf{v}_k = \sum_{j=1}^{N-1} \mu_j^k \boldsymbol{\zeta}_j$ for $k = 1, \dots, N-1$, then $[\mathbf{v}_1, \dots, \mathbf{v}_{N-1}] = V_1^{N-1} = \Xi Y$, where the elements $\boldsymbol{\zeta}_j$ of Ξ are given by $\Xi = V_1^{N-1} Y^{-1}$. Introducing the next snapshot

$$\mathbf{v}_N = \sum_{j=1}^{N-1} \mu_j^{N-1} \boldsymbol{\zeta}_j + \mathbf{r}, \qquad \mathbf{r} \perp \operatorname{span}\{\mathbf{v}_1, \dots, \mathbf{v}_{N-1}\}$$

one has

$$V_2^N = V_1^{N-1} C + \mathbf{r}\mathbf{e}^T = V_1^{N-1} Y^{-1} \Lambda Y + \mathbf{r}\mathbf{e}^T = \Xi \Lambda Y + \mathbf{r}\mathbf{e}^T.$$

- → If $\mathbf{r} = \mathbf{0}$: the approximate modes are indistinguishable from Koopman modes.
- → If $\mathbf{r} \neq \mathbf{0}$: $(\mu_j, \boldsymbol{\zeta}_j)$ are approximations of the eigenvalues and Koopman modes (scaled by $\varphi_j(\mathbf{X}_0)$).

DMD algorithm

$[\mathbf{Z}, \mu, \mathrm{Res}] = \mathrm{DMD}\left(V_1^N\right)$
Input : N sequence of snapshots $V_1^N = \{\mathbf{v}_1, \mathbf{v}_2, \mathbf{v}_3, \cdots, \mathbf{v}_N\}$
Output : $(N-1)$ empirical Ritz vectors $\mathbf{Z}$ and Ritz values μ ; Res : residual.

- $m = \mathrm{size}\left(V_1^N, 1\right)$
- $N = \mathrm{size}\left(V_1^N, 2\right)$
- $\mathbf{v}_N = V_1^N(:, N)$
- $V_1^{N-1} = V_1^N(:, 1 : N-1)$
- $V_2^N = V_1^N(:, 1 : N-1)$
- $\mathbf{c} = V_1^{N-1} / \mathbf{v}_N$
- $S = \mathrm{companion}\left(\mathbf{c}\right)$
- $[Y, \mu] = \mathrm{eig}(S)$
- $Z = V_1^{N-1} Y$
- $\mathrm{Res} = \mathrm{norm}\left(V_2^N - V_1^{N-1} S, 1\right)$

with $Z = (\mathbf{z}_1, \cdots, \mathbf{z}_N)$ and $Y = (\mathbf{y}_1, \cdots, \mathbf{y}_N)$.

Preprocessing of the data

- Apply the SVD

$$V_1^{N-1} = \Psi \Sigma \Phi^H \qquad \text{with} \qquad \Psi\Psi^H = I_{m\times m},\ \Phi\Phi^H = I_{N\times N}$$

Remarks :

- Ψ contains the spatial POD eigenfunctions and,
- Φ contains the temporal POD eigenfunctions

POD is here a by-product of DMD

- Starting from $AV_1^{N-1} = V_1^{N-1}S + \mathbf{r}\mathbf{e_{N-1}}^T$ and first considering that $\mathbf{r} = \mathbf{0}$, we obtain after some manipulations :

$$\Psi^H A \Psi = \Psi^H V_2^N \Phi \Sigma^{-1} = S$$

Since $\mathbf{r} \neq \mathbf{0}$, we have :

$$\boxed{\Psi^H A \Psi = \Psi^H V_2^N \Phi \Sigma^{-1} = \tilde{S}} \qquad \text{where} \qquad \tilde{S} \quad \text{is a full matrix.}$$

Ritz eigenvalues

- If we already know eigen-elements of $\tilde{S}$ then we can determine approximated eigen-elements of A. Indeed :

$$\boxed{\text{if} \quad \tilde{S}\mathbf{y_i} = \mu_i \mathbf{y_i} \qquad \text{then} \qquad A\boldsymbol{\xi}_i = \mu_i \boldsymbol{\xi}_i \quad \text{with} \quad \boldsymbol{\xi}_i = \Psi \mathbf{y_i}}$$

Proof :

$$\begin{aligned} A\boldsymbol{\xi}_i = \mu_i \boldsymbol{\xi}_i \quad & \Rightarrow A\Psi\mathbf{y_i} = \mu_i \Psi \mathbf{y_i} \\ & \Rightarrow \Psi^H A \Psi \mathbf{y_i} = \mu_i \Psi^H \Psi \mathbf{y_i} = \mu_i \mathbf{y_i} \\ & \Rightarrow \tilde{S}\mathbf{y_i} = \mu_i \mathbf{y_i} \end{aligned}$$

DMD applied to the cylinder wake flow

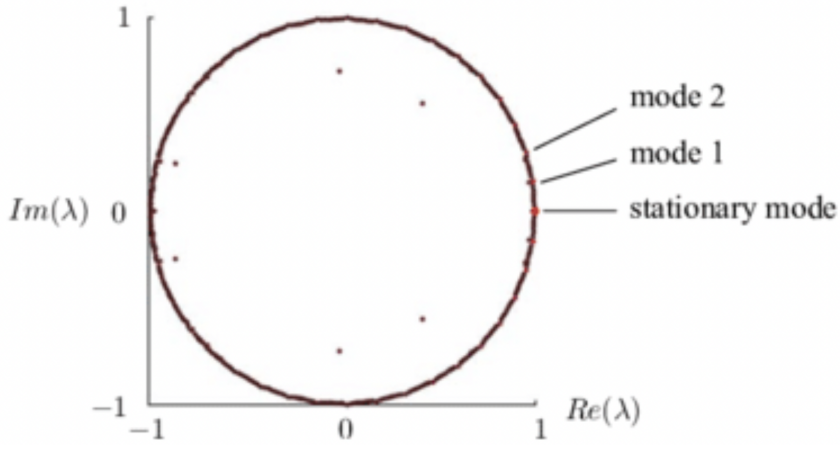

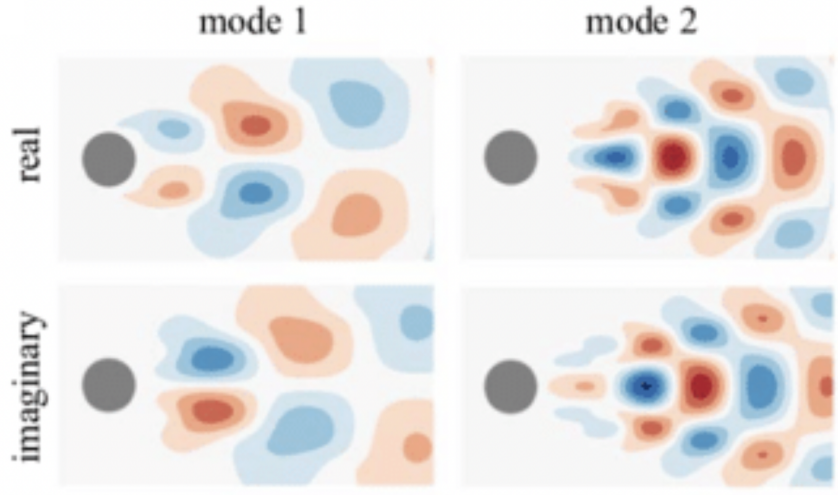

Dynamic modes of an unstable jet flow

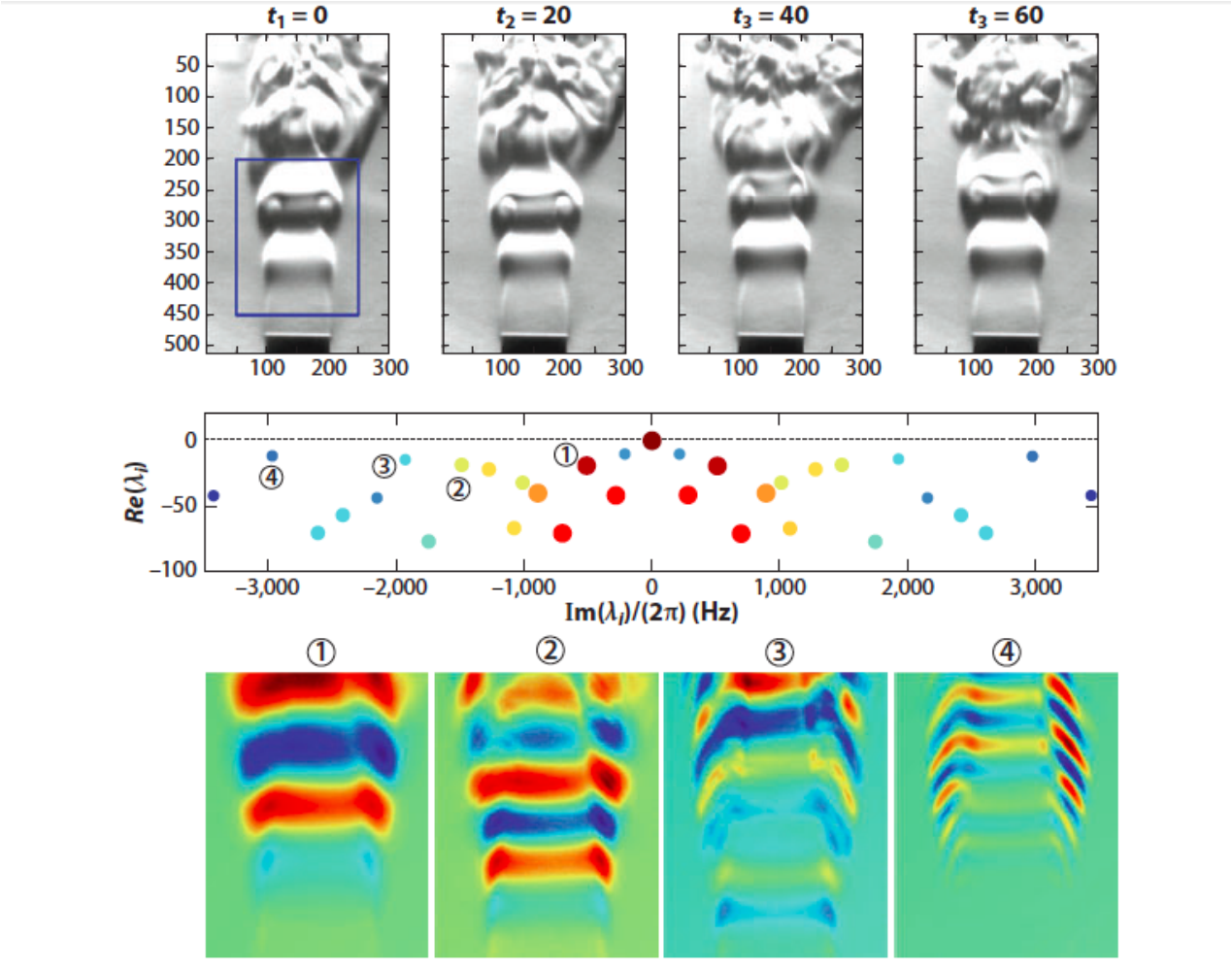

Figure 6

(*Top panel*) Time evolution of a low-density helium jet. (*Middle panel*) Koopman spectrum obtained using an Arnoldi algorithm. Larger symbols correspond to larger-scale structures, and smaller ones to smaller-scale structures. (*Bottom panel*) Four Koopman modes, whose eigenvalues are numbered in the middle panel. Figure taken from Schmid et al. (2011).

DMD applied to a jet in cross-flow

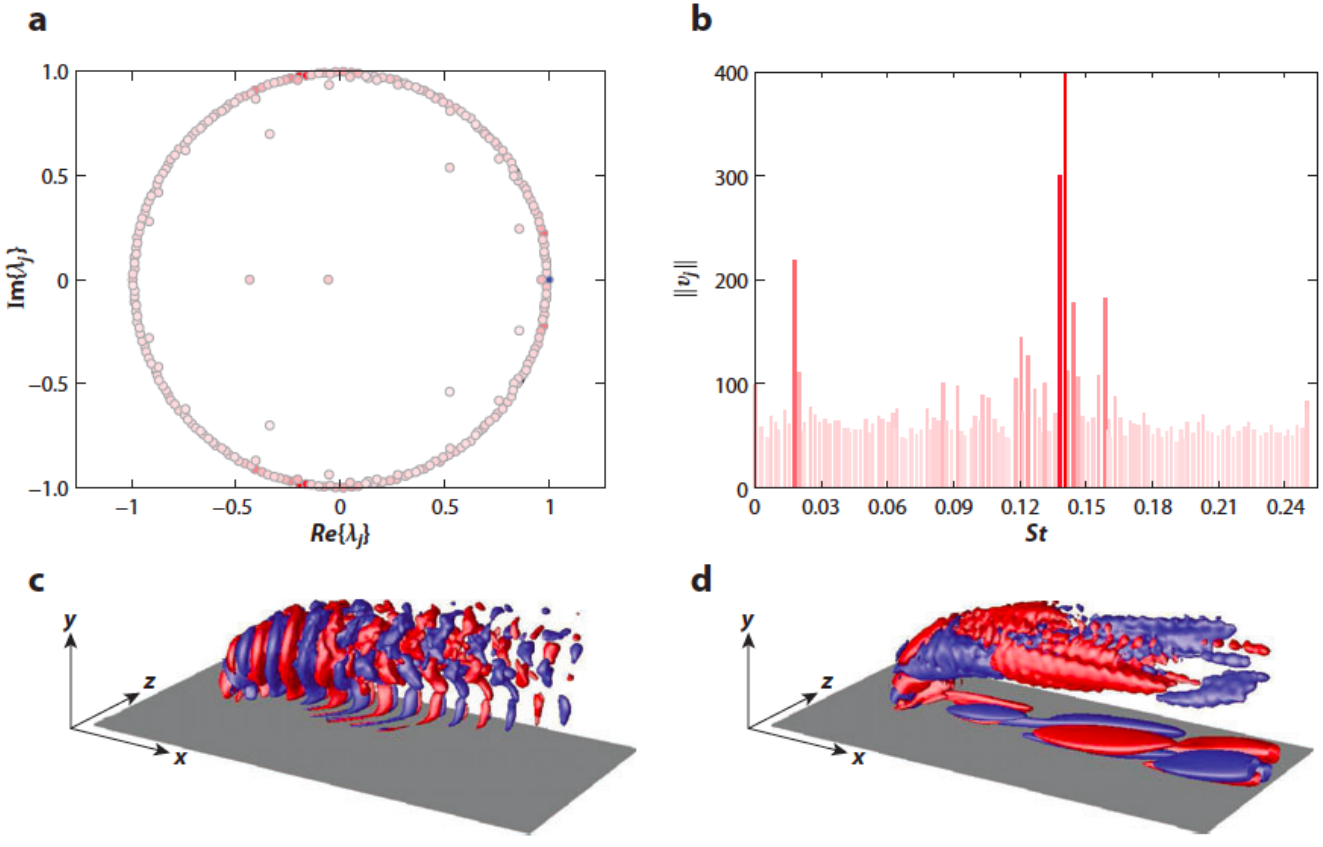

Figure 3

(*a*,*b*) Part of the spectrum of the Koopman operator for a jet in crossflow, with (*a*) Koopman eigenvalues on the unit circle, with the darker red indicating a larger Koopman mode amplitude and blue indicating eigenvalue 1, and (*b*) their magnitudes. (*c*,*d*) The two largest magnitude Koopman modes corresponding to (*c*) high and (*d*) low frequency. Positive (*red*) and negative (*blue*) contour levels of the streamwise velocity components of two Koopman modes are shown. The direction of the crossflow is *z*. Figure taken from Rowley et al. (2009).

I. Mezić, Annu. Rev. Fluid Mech. 45 (2013) 357-78

POD vs DMD

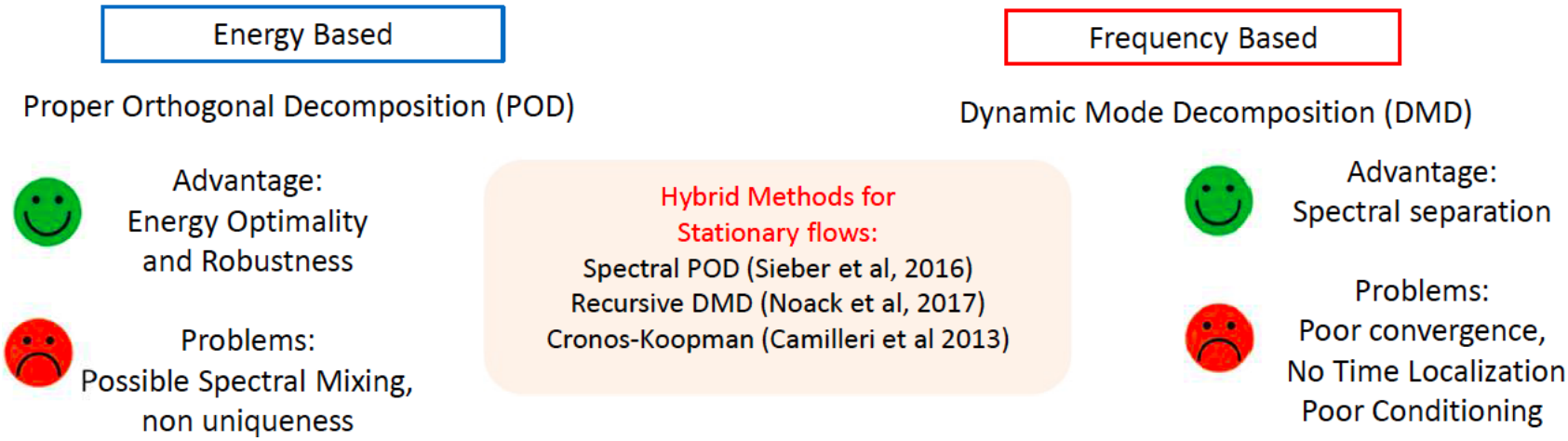

from M.A. Mendez, Fundamentals and Recent Advances in Particle Image Velocimetry and Lagrangian Particle Tracking, VKI lecture series, Nov. 2021.

Bibliography

- L. Cordier, Workshop "Flow Control Methods and Application", Poitiers, December 7-11, 2009
- G. Berkooz, Gal, P. Holmes, & J.L. Lumley. "The proper orthogonal decomposition in the analysis of turbulent flows." Annual review of fluid mechanics 25 (1993) 539-575.
- P.J. Schmid, "Application of the dynamic mode decomposition to experimental data", Experiments in fluids, 50 (2011) 1123-1130.
- P.J. Schmid, "Dynamic mode decomposition of numerical and experimental data", Journal of fluid mechanics 656 (2010) : 5-28.
- C.W. Rowley, I. Mezić, S. Bagheri, P. Schlatter & D.S. Henningson. "Spectral analysis of nonlinear flows", J. of Fluid Mech. 641 (2009) 115-127.
- I. Mezić, "Analysis of fluid flows via spectral properties of the Koopman operator", Annual Review of Fluid Mechanics 45 (2013) 357-378.

To go further :

- P. Holmes, J.L. Lumley, G. Berkooz, G., & C.W. Rowley, "Turbulence, coherent structures, dynamical systems and symmetry". Cambridge university press, 2012.
- Aaron Towne, Oliver T. Schmidt & Tim Colonius, "Spectral proper orthogonal decomposition and its relationship to dynamic mode decomposition and resolvent analysis", J. Fluid Mech. (2018), 847, pp. 821-867.